JCB Article

Trafficking of prion proteins through a caveolae-mediated endosomal pathway

Peter J. Peters,[1,2,3] Alexander Mironov, Jr.,[1] David Peretz,[4,5] Elly van Donselaar,[3] Estelle Leclerc,[8] Susanne Erpel,[4,5] Stephen J. DeArmond,[4,6] Dennis R. Burton,[8] R. Anthony Williamson,[8] Martin Vey,[4,5] and Stanley B. Prusiner[4,5,7]

[1]Section of Tumor Biology, Netherlands Cancer Institute, 1066 CX Amsterdam, Netherlands
[2]Department of Molecular Cell Biology, Free University, 1081 BT Amsterdam, Netherlands
[3]Department of Cell Biology, Faculty of Medicine, Utrecht University, 3584 CX Utrecht, Netherlands
[4]Institute for Neurodegenerative Diseases, [5]Department of Neurology, [6]Department of Pathology, and [7]Department of Biochemistry and Biophysics, University of California, San Francisco, CA 94143
[8]Department of Immunology, Scripps Research Institute, La Jolla, CA 92037

To understand the posttranslational conversion of the cellular prion protein (PrP^C) to its pathologic conformation, it is important to define the intracellular trafficking pathway of PrP^C within the endomembrane system. We studied the localization and internalization of PrP^C in CHO cells using cryoimmunogold electron microscopy. At steady state, PrP^C was enriched in caveolae both at the TGN and plasma membrane and in interconnecting chains of endocytic caveolae. Protein A–gold particles bound specifically to PrP^C on live cells. These complexes were delivered via caveolae to the pericentriolar region and via nonclassical, caveolae-containing early endocytic structures to late endosomes/lysosomes, thereby bypassing the internalization pathway mediated by clathrin-coated vesicles. Endocytosed PrP^C-containing caveolae were not directed to the ER and Golgi complex. Uptake of caveolae and degradation of PrP^C was slow and sensitive to filipin. This caveolae-dependent endocytic pathway was not observed for several other glycosylphosphatidyl inositol (GPI)-anchored proteins. We propose that this nonclassical endocytic pathway is likely to determine the subcellular location of PrP^C conversion.

Introduction

Prion diseases are fatal neurodegenerative disorders. Transmission studies using transgenic and PrP-ablated (*Prnp*$^{0/0}$) mice have shown that disease is caused by the abnormally folded prion protein (PrP^{Sc}) (Prusiner, 1994). PrP^{Sc} is formed from a glycosylphosphatidyl inositol (GPI)–anchored, protease-sensitive cellular isoform (PrP^C) by a posttranslational refolding process (Oesch et al., 1985; Borchelt et al., 1990; Caughey and Raymond, 1991). During refolding, regions of the primarily α-helical PrP^C molecules are converted to β-helical structures (Pan et al., 1993, Wille et al., 2002). After conversion, PrP^{Sc} accumulates in a late endocytic lysosomal compartment of the infected cell (Taraboulos et al., 1990; McKinley et al., 1991; Arnold et al., 1995). The mechanism involved in the conversion of PrP^C to PrP^{Sc} and the exact subcellular site of PrP^{Sc} formation have not yet been determined.

Posttranslational GPI anchoring, disulfide bonding, and glycosylation of PrP^C in the ER direct PrP^C through the Golgi complex into the post-Golgi, cholesterol-rich, caveolae-like domains (CLDs) (Vey et al., 1996). Caveolae, specialized membrane microdomains that contain members of the caveolin protein family, are rich in cholesterol and glycosphingolipids and often appear as flask-shaped invaginations on the plasma membrane or form more complex interconnected chains of several caveolae with a single neck connecting the chains to the outer surface of the cell (Parton, 2003). Caveolae mediate a number of key physiological processes, such as signal transduction and transcytosis (Anderson, 1998; Kurzchalia

The online version of this article includes supplemental material.

Address correspondence to Peter J. Peters, Netherlands Cancer Institute, Antoni van Leeuwenhoek Hospital, Plesmanlaan 121-H4, 1066 CX Amsterdam, The Netherlands. Tel.: 31-20-512 2989. Fax: 31-20-617-2029. email: p.peters@nki.nl.

M. Vey's present address is Aventis Behring GmbH, Marburg, Germany.

Key words: prion; caveolae; endosomal pathway; electron microscopy; cryoimmunogold

Abbreviations used in this paper: CLD, caveolae-like domain; GPI, glycosylphosphatidyl inositol; PIPLC, phosphatidylinositol-specific phospholipase C; PrP^C, cellular isoform of the prion protein; PrP^{Sc}, disease-causing isoform of the prion protein.

Supplemental material can be found at:
http://doi.org/10.1083/jcb.200304140

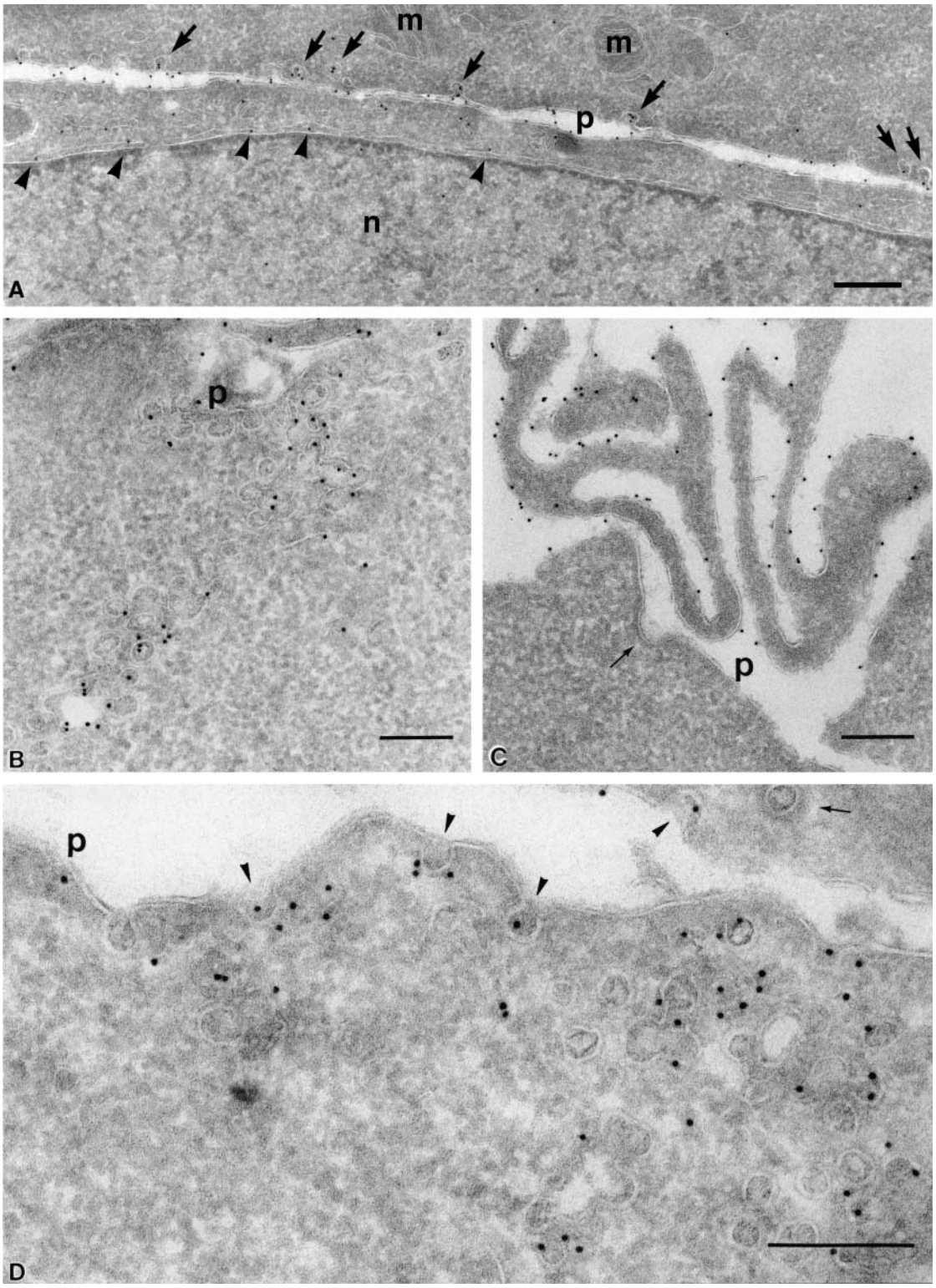

Figure 1. **At steady state, PrP^C is enriched in lamellae and caveolae both at the plasma membrane and inside the cell.** (A–C) PrP^C was immunogold labeled on ultrathin cryosections of CHO/30C3 cells (steady-state distribution of PrP^C) using the R1 recombinant antibody Fab fragment against PrP^C. Labeling was observed on the ER (A, arrowheads), plasma membrane caveolae-like structures (A, arrows), caveolae-like structures that appeared as flask-shaped invaginations on the plasma membrane (p) and interconnecting chains of caveolae-like structures deeper into the cytoplasm (B), and microvilli at the leading edge of the cell (C). Clathrin-coated pits (C, thin arrow) did not label. (D and E) Caveolin-1 was immunogold labeled on ultrathin cryosections of CHO/30C3 cells using anti-caveolin-1–gold labeling. (D) Caveolae-like structures and interconnecting chains of caveolae-like structures deeper into the cytoplasm labeled with a caveolin-1 antibody under steady-state conditions. (E) Protein A–gold uptake in an $SHaPrP^C$-expressing cell, after a 10-min pulse. Gold labeling was observed on the plasma membrane and was enriched in caveolae (arrowheads). (F) After a 10-min pulse and 50-min chase, gold labeling was observed in small vesicles near the Golgi complex and lysosomes. G, Golgi complex; l, lysosomes; m, mitochondria; n, nucleus; p, plasma membrane. Bar, 200 nm (applies to all panels).

and Parton, 1999; Brown and Jacobson, 2001; Conner and Schmid, 2003; Parton, 2003). CLDs, also called lipid rafts (Simons and Ikonen, 1997), are biochemically defined in terms of their Triton X-100 detergent insolubility at 4°C. Caveolae can be considered a special class of raft. However, because Triton insolubility is also considered the standard hallmark of cytoskeletal association of membrane proteins (Scherfeld et al., 1998), one cannot assume that CLDs are equivalent to purified caveolae.

CLDs appear to be crucial to the PrP^{C}-to-PrP^{Sc} conversion process (Taraboulos et al., 1995; Vey et al., 1996; Kaneko et al., 1997; Naslavsky et al., 1997). PrP^{C} with modifications in the cytoplasmic tail, which cause it to be redirected to clathrin-coated pits, is not converted to PrP^{Sc} (Taraboulos et al., 1995; Kaneko et al., 1997). Significantly, neurons in culture (Mouillet-Richard et al., 2000), astrocytes, and basal ganglion cells contain caveolae, raising the possibility that PrP^{C} resides in these structures. In addition, many different caveolae-containing cell types outside the nervous system that express PrP^{C} may be required for the transmission of prion diseases.

Here we report on the trafficking of PrP^{C} in CHO cells stably transfected with either Syrian hamster (SHa) or chimeric mouse–hamster (MH2M) PrP^{C} using cryoimmunogold electron microscopy. We found that PrP^{C} was highly enriched in the caveolae and caveolae-containing endocytic structures of these cell lines.

Results

PrP^{C} expression levels do not interfere with caveolin-1 expression in CHO cells

Previous studies demonstrating Triton X-100 detergent insolubility of PrP^{C} in neuroblastoma (N2a) cells have suggested that PrP^{C} is concentrated in CLDs (Ying et al., 1992; Gorodinsky and Harris, 1995; Harmey et al., 1995; Vey et al., 1996; Naslavsky et al., 1997). However, these studies are complicated by the dramatically disparate caveolin levels found in dif-

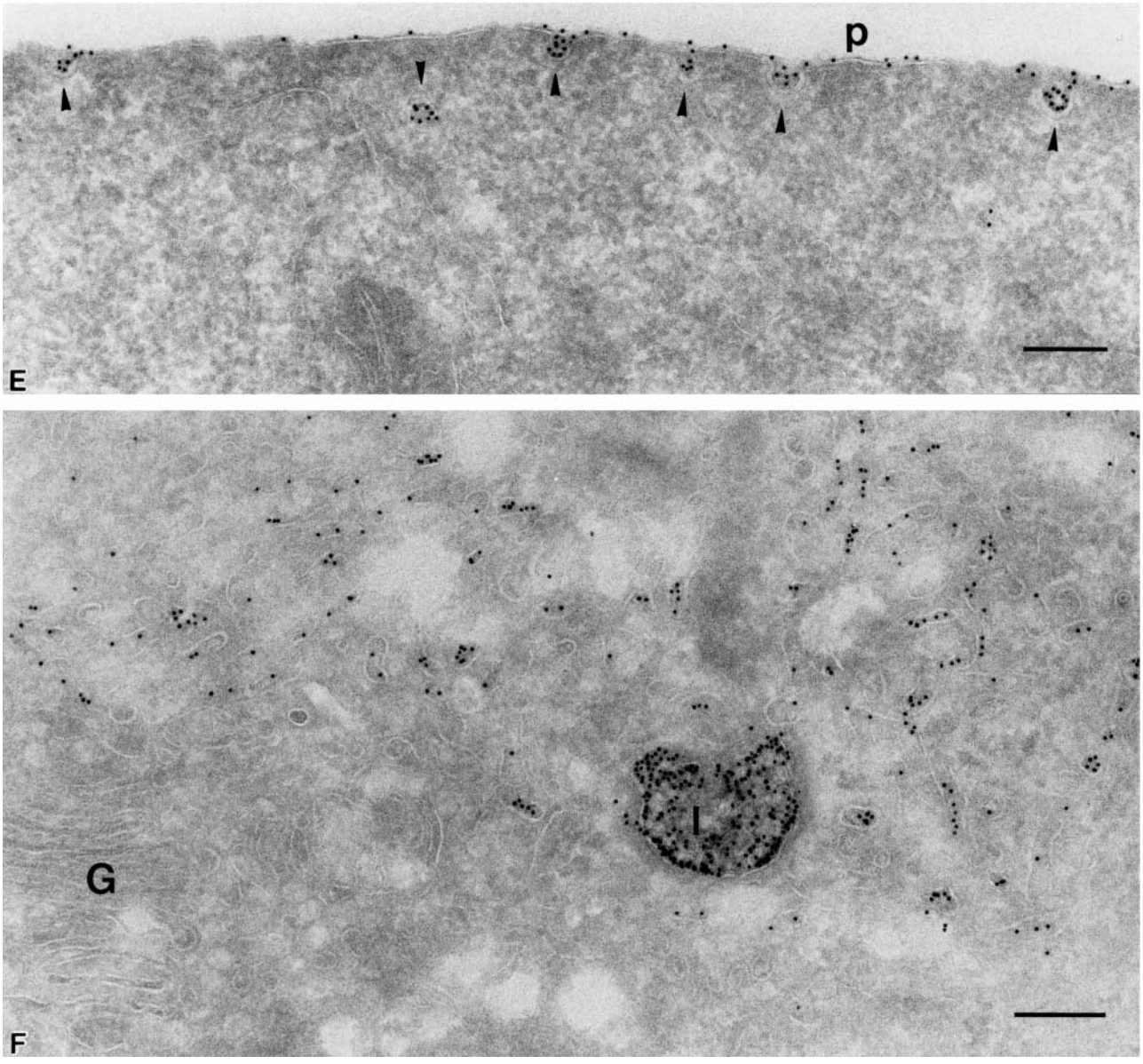

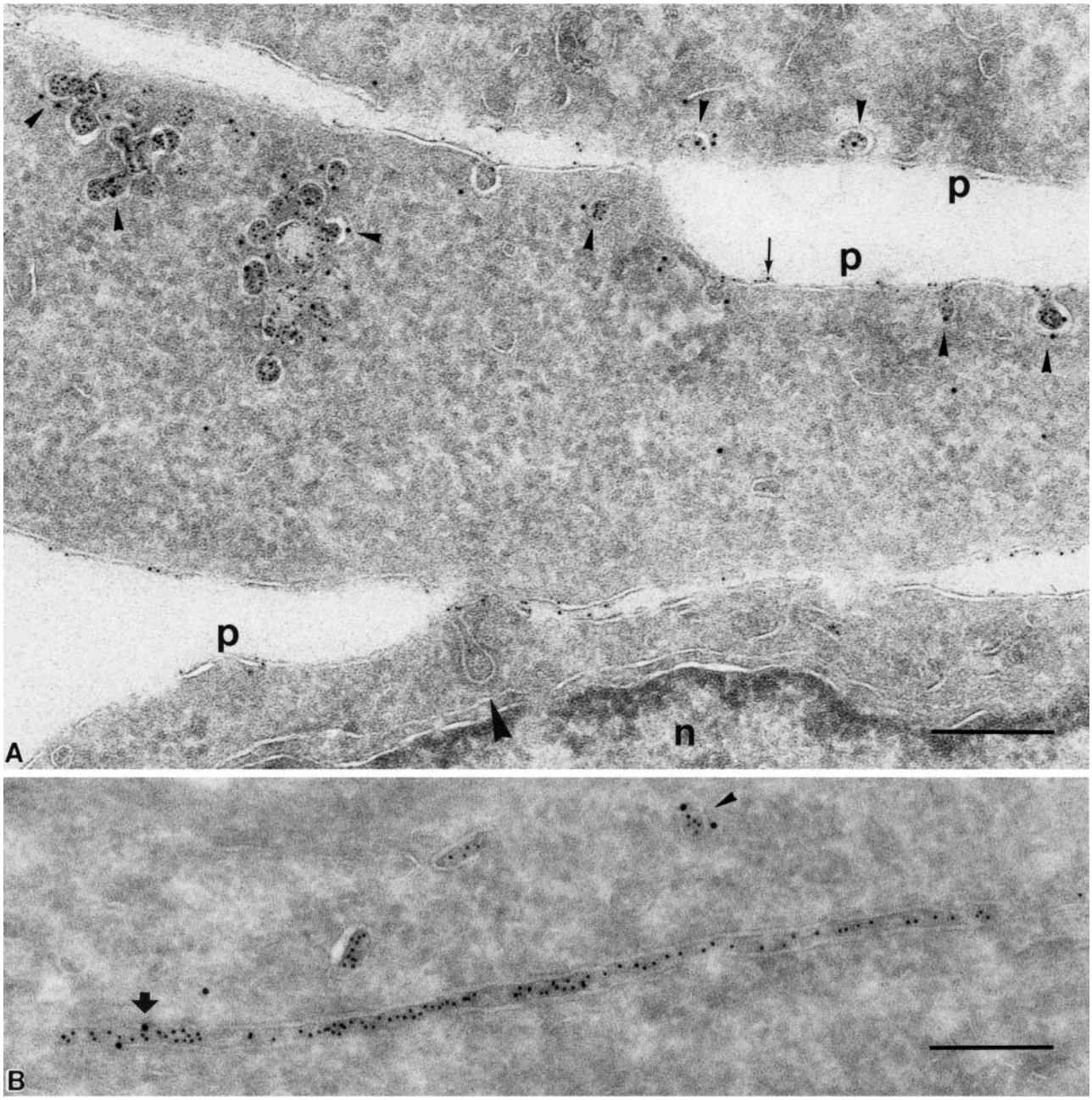

Figure 2. **PrP^C is internalized into nonclassical endosomes via caveolae, and this internalization is triggered by surrogate ligand protein A–gold.** (A) Endocytosed protein A–gold is found in caveolae of SHaPrP^C-expressing CHO/30C3 cells. Cells were incubated at 37°C for 10 min with protein A–gold (5 nm) and chased for 50 min before fixation. Ultrathin cryosections were labeled with anti–caveolin-1 (10-nm gold). Protein A–gold (5 nm) detecting PrP^C labeling was observed on the plasma membrane (thin arrow) and was enriched in caveolae (arrowheads) and caveolin-1–positive (10-nm gold) structures. Clathrin-coated pit (large arrowhead) did not label for either PrP^C or caveolin-1. (B) Tubule and vesicular structures (small arrowhead) that contained endocytosed protein A–gold (5 nm) labeled for caveolin-1 (10 nm, large arrow). (C) Caveolae (caveolin-1, 10 nm, thick arrows) were present on endocytic structures that were enriched for endocytosed protein A–gold (5-nm gold, small gold, thin arrows). Protein A–gold (5 nm) was also present on the plasma membrane (arrowhead). Panel D depicts an endocytic structure loaded with endocytosed protein A–gold (5 nm, thin arrows) with fused caveolae (thick arrows) labeled for caveolin-1 (10-nm gold) surrounded by caveolae (arrowheads) at the pericentriolar region of the cell that also labeled for caveolin-1 (10 nm) and contained endocytosed protein A–gold (5 nm). Compared with C, the endocytic structure shown contained caveolae that have less caveolar appearance, as if they were fused with the endosome. (E) Endocytosed protein A–gold (5 nm) was present exclusively on the plasma membrane, on plasma membrane–associated caveolae (caveolin-1, 10 nm, arrowheads), and in lysosomes (thin arrows show caveolin-1 label, 10-nm gold). The Golgi complex, labeled for caveolin-1 in a nonclustered fashion, did not contain endocytosed protein A–gold (5 nm). Clathrin-coated pit (thick arrow), nuclear envelope–ER, and clathrin-coated vesicles (not depicted) did not exhibit endocytosed protein A–gold. c, centriole; e, endocytic structure; G, Golgi complex; l, lysosome; m, mitochondria; n, nucleus; p, plasma membrane. Bar, 200 nm (applies to all panels).

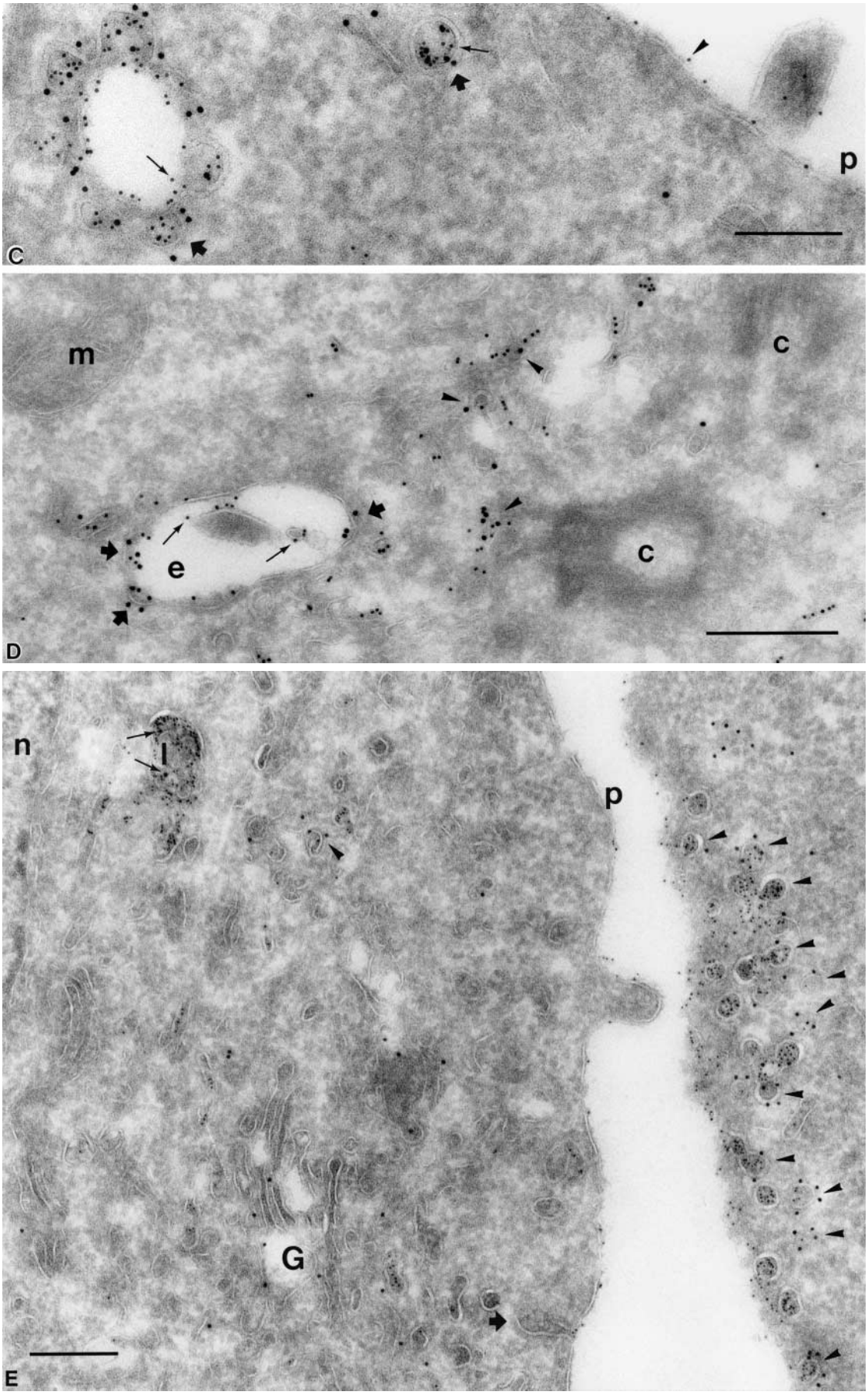

ferent N2a cells (Ying et al., 1992; Gorodinsky and Harris, 1995; Harmey et al., 1995). To determine the expression levels of caveolin in the CHO cells used in our experiments, we performed Western blotting to measure levels of both PrP^C and caveolin-1. Immunoblotting revealed that CHO/30C3 and CHO/MH2M cell lines express $SHaPrP^C$ and $MH2MPrP^C$, respectively. Neither the parental, nontransfected CHO/K1 line nor the cell line expressing the empty vector (CHO/EV) showed a PrP^C signal when probed with the 3F4 mAb specific for $SHaPrP^C$ and $MH2MPrP^C$ (unpublished data). In addition, these cells did not express detectable amounts of endogenous PrP^C when analyzed with the polyclonal antiserum RO73 that recognizes PrP^C (unpublished data). When probed with a polyclonal α-caveolin-1 antibody, all cell lines were found to express equal levels of caveolin-1 (unpublished data). These results indicate that CHO cells express caveolin and that the overexpression of $SHaPrP^C$ or $MH2MPrP^C$ did not alter the levels of caveolin. Because the results described below were indistinguishable for cells expressing $SHaPrP^C$ and those expressing $MH2MPrP^C$, only the results for CHO/30C3 cells expressing $SHaPrP^C$ are presented.

PrP^c is present in caveolae

To determine whether PrP^C and caveolin-1 reside in caveolae in CHO cells, we analyzed the distribution of these proteins on ultrathin cryosections. Sections of 30C3 cells were labeled with anti-PrP^C Fab R1. Anti-PrP^C label was present on the nuclear envelope and ER (Fig. 1 A), Golgi complex (see Fig. S1 A, available at http://www.jcb.org/cgi/content/full/jcb.200304140/DC1), non–clathrin-coated tubules/vesicles in the TGN around the pericentriolar region (Fig. S1 B) and plasma membrane (Fig. 1 A and Fig. S1 C), and in multivesicular late endocytic structures (Fig. S1 F). Intense labeling for PrP^C was detected in structures resembling caveolae (Fig. 1 A and Fig. S1 D) and at the edges of the leading lamellae and ruffles of the plasma membrane (Fig. 1 C and Fig. S1 C), interconnecting chains of caveolae-type structures near the plasma membrane (Fig. 1 B and Fig. S1 D), and far from the plasma membrane (Fig. S1 E). Both the nucleus and mitochondria exhibited very little background label. No noticeable gold particles were found in clathrin-coated pits and vesicles at the plasma membrane (Fig. 1 C; Fig. 2, A and E; and Fig. S1 D) and TGN (Fig. S1 B), suggesting that PrP^C was not transported via clathrin-coated pits. This pattern of labeling was specific because the parental CHO/K1 and CHO/EV cells that do not express PrP^C did not exhibit any PrP^C label (unpublished data). In addition, identical labeling was generated with R2, D13, and D18, three other recombinant Fabs raised against other regions of PrP (unpublished data). Importantly, all the antibodies labeled PrP^C in glutaraldehyde-fixed cells, a treatment that, in contrast to paraformaldehyde alone, does not allow lateral movement of GPI-anchored proteins in the lipid bilayer and therefore prevents artificial molecular clustering in membrane domains (Madore et al., 1999).

Immunogold labeling of caveolin-1 was found in cryosections of all cell lines irrespective of PrP^C expression. In CHO/30C3 cells, gold particles were found almost exclusively decorating 40–50-nm invaginated structures on the plasma membrane and internal compartments of similar dimensions (Fig. 1 D and Fig. 2, A and C–E). Gold particles for caveolin-1 and PrP^C were seen on both the luminal and cytosolic sides of the membrane. This observation is unlikely to indicate the presence of caveolin-1 and PrP^C on both sides of the membrane, but results from a previously described phenomenon in which the antibody and protein A–gold complex traverse the 20-nm phospholipid membrane bilayer. Based on these data, we conclude that PrP^C is enriched in lamellae and caveolae both at the plasma membrane and inside the cell.

Protein A–gold particles bind to cells expressing PrP^C

In experiments designed to determine whether the interconnecting chains of caveolae-type structures that are far removed from the plasma membrane (Fig. S1 E) are of endocytic origin, we used gold probes as markers for the endocytic pathway. We observed, to our surprise, that protein A affinity coupled to gold particles bound PrP^C-expressing cells. All cell pellets that were analyzed for EM exhibited an intense red color (the color of the gold probe), whereas the control cells remained white (see Fig. S2 E, available at http://www.jcb.org/cgi/content/full/jcb.200304140/DC1).

To determine whether protein A–gold binds to PrP^C specifically, we performed a series of biochemical experiments in which we compared protein A–gold with IgG-coated gold and with protein A coupled with FITC. Binding of labeled conjugates was performed on the different cells in culture and on purified proteins immobilized on nitrocellulose. Confluent cells were incubated with protein A–gold, IgG–gold, or protein A coupled to FITC for 1 h. PrP^C-expressing cells bound protein A–gold (Fig. 1 E) but did not bind to either IgG–gold by electron microscopy or protein A–FITC by fluorescence microscopy. Neither CHO/K1 nor CHO/EV cells that do not express $SHaPrP^C$ bound protein A (Table I).

Table I. **Binding studies using different labeling reagents**

Cells	Protein A–gold[a]	Goat IgG–gold[a]	Protein A–FITC[a]
CHO/30C3	+	−	−
CHO/MH2M	+	−	−
CHO/EV	−	−	−
CHO/K1	−	−	−
$SHaPrP^C$ (brain derived)	+	ND	ND
$SHaPrP^C$ (30C3)	+	ND	ND
BSA	−	ND	ND

[a]+, binding; −, no binding.

To determine whether purified PrP^C binds to protein A–gold, we transferred 8 μg of $SHaPrP^C$ isolated from hamster brain or from CHO/30C3 cells to nitrocellulose and measured the binding of protein A. $SHaPrP^C$ from brain and CHO/30C3 cells, but not the control BSA, gave a specific signal (Table I). To demonstrate unambiguously, via an independent method, that protein A–gold binds specifically to PrP^c under native conditions in living cells, we preincubated $SHaPrP^C$-expressing cells with and without the anti-PrP Fab cocktail mix (R1, D13, and D18). This was followed by sheep anti–mouse Fab that covered the anti-PrP antibodies. Sheep anti–mouse does not bind directly to PrP^C. PrP^C-expressing cells that were treated with the cocktail and then incubated in media containing protein A–gold remained white (unpublished data). Apparently, the anti-PrP mouse antibodies masked the PrP^C epitope on the living CHO cells and thus prevented protein A–gold particles from binding. Based on these findings, we conclude that $SHaPrP^C$ bound protein A–gold in a specific manner and that no other surface proteins in CHO cells bound to protein A–gold. We have not tested whether any other PrP^C from other species reacted with protein A–gold.

PrP^C is endocytosed via caveolae

To investigate the intracellular fate of protein A–gold label in cells expressing PrP^C, we performed a series of uptake experiments. Protein A–gold was added to the cells for 10 min, followed by a wash with or without a chase in medium for 50 min, all performed at 37°C, after which the cells were fixed. We observed that after the 10-min incubation, protein A–gold was highly concentrated in 50-nm coated pits that were morphologically indistinguishable from caveolae (Fig. 1 E, arrowheads). After the 10-min incubation and 50-min chase, many (non–clathrin-coated) tubulo-vesicular structures in the pericentriolar region were loaded with protein A–gold. In addition, accumulation of gold label was seen in multivesicular-type, relatively round structures without tubular extensions and ~200–300 nm in size, features indicative of late endosomal/lysosomal structures (Fig. 1 F). Later in this study, we found that these structures contained the lysosomal glycoprotein LGP120. Mitochondria, ER, and Golgi complex (Fig. 1, E and F) were devoid of label. These observations suggest that the PrP^C–protein A–gold complexes had entered the cells via caveolae before they were transported to lysosomes.

To confirm that endocytosed protein A–gold particles were indeed present in caveolae, we labeled the cryosections from the 10-min pulse with anti–caveolin-1 antibodies. All structures loaded with endocytosed protein A–gold particles also labeled for caveolin-1 (Fig. 2, A–E, large gold), thus confirming their caveolar origin. The apparent lack of PrP^C label on clathrin-coated pits (Fig. 2 A) precludes the possibility of internalization via this pathway. Interestingly, we occasionally found long tubular profiles loaded with endocytosed protein A–gold that also labeled for caveolin-1 (Fig. 2 B), illustrating that the endocytosed caveolar compartment has a tubular component.

Because endocytosed protein A–gold particles accumulated in late endosomal/lysosomal structures, we searched for an endocytic intermediate in the endosomal pathway. We found vacuolar structures (Fig. 2 C) resembling endosomes that had accumulated the endocytosed protein A–gold (thin arrows). Compared with control cells (Fig. S1 E) where one can observe PrP^C under steady-state conditions in endocytic structures, these structures appeared more swollen. Interestingly, these swollen endocytic intermediates were also decorated with caveolae and stained positively for caveolin-1. Even in the pericentriolar region, endocytosed protein A–gold particles were present in caveolae that label with caveolin-1 (Fig. 2 D). In addition, fusion profiles of caveolae with endosomes were observed (Fig. 2 D), while the endocytosed protein A–gold particles were deposited within the lumen of the endosome (small arrows). To search for resident molecules of these "rosettes" of endocytic caveolae, we tried labeling for different markers. Neither EEA1, Rab 4, nor Rab 5 labeled on these structures, and transferrin receptor did not colocalize. Thus, only the exogenously provided protein A–gold was detectable within the compartment in the section, and the presence of small (50 nm) vesicles within these 200–300-nm structures was used as a criterion to determine their endocytic origin. To provide further evidence that under steady state, caveolae-containing endocytic structures exist, we incubated the cells at 4°C with protein A–gold and found similar profiles devoid of protein A–gold but positive for caveolin-1 (later in this study). We conclude that these endocytic structures are nonclassical.

We next addressed whether caveolin-1 would remain in these structures during the endocytic process toward late multivesicular endosomes/lysosomes. To make this determination, we evaluated whether caveolin-1 and protein A–gold were present in multivesicular structures characteristic of late endosomal/lysosomal structures. Cells were pulsed with protein A–gold for 10 min, chased for 50 min, and then sectioned and labeled with anti–caveolin-1. All late endosomal/lysosomal structures that were loaded with endocytosed protein A–gold also labeled for caveolin-1 (Fig. 2 E). At least two to three gold particles per late endosomal/lysosomal structure that labeled with caveolin-1 (Fig. 2 E, thin arrows) were usually present on membranes within the multivesicular/membranous lysosomal compartment, suggesting lysosomal delivery of caveolin. This phenomenon was also seen before the uptake experiment (unpublished data), suggesting a possible involvement of the endosomal/lysosomal pathway for caveolin degradation.

To evaluate whether protein A–gold remains bound to PrP^C in the downstream endocytic compartments, we asked whether the presence of endocytosed protein A–gold always correlates with the relative intensity and distribution of PrP^C on ultrathin cryosections using anti-PrP^C–gold (Fig. 1, A–C, and Fig. S1, C–F). To address this question, we labeled the ultrathin cryosections similar to those that were analyzed in Fig. 1 (E and F) (10-min uptake of protein A–gold and 10-min uptake plus 50-min chase) with anti-PrP^C mouse antibody D18 and compared the relative distribution of this label with the endocytosed protein A–gold. We analyzed 20 random cross sections and quantified the ratio of the 10-min protein A–gold uptake. The ratio of small (10-nm) protein A–gold probe to large (15-nm) anti-PrP^C–gold remained identical at the leading edge and within caveolae-type endocytic structures (Fig. S2 A). An identical correlation was also found between a small (5-nm) protein A–gold probe and a large (15-nm) anti-PrP^C–gold.

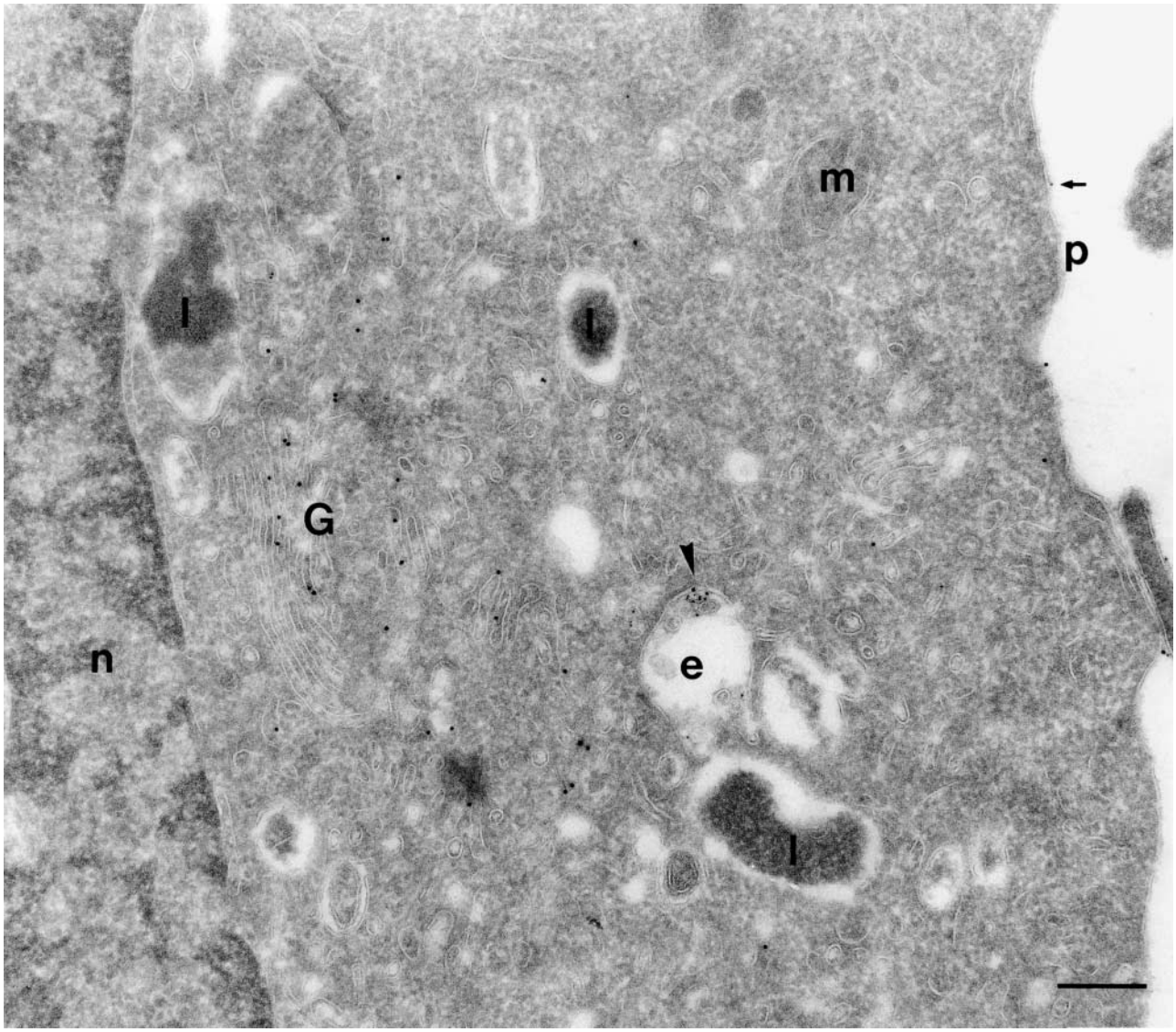

Figure 3. **PIPLC treatment of SHaPrP^C-expressing CHO/30C3 cells inhibited PrP^C-dependent protein A–gold uptake.** Cells expressing PrP^C were treated with PIPLC for 2 h and incubated with protein A–gold (5 nm; 10-min pulse and 50-min chase during the last hour of enzyme digestion) before fixation. Sections were labeled for PrP^C using the R1 Fab. Only a very small fraction of the protein A–gold (small gold, arrowhead) was endocytosed. Only a few (arrow) protein A–gold particles, but no PrP^C labeling (10-nm gold), were observed on the plasma membrane. However, abundant labeling for PrP^C was seen in the Golgi. e, endocytic structure; G, Golgi complex; l, lysosome; n, nucleus; m, mitochondria; p, plasma membrane. Bar, 200 nm.

However, relatively more small (5-nm) gold was present due to its much higher binding efficiency. When the caveolae and interconnecting caveolae (Fig. S2 B) and late endocytic multivesicular profiles (Fig. S2 C) were analyzed, we again found a strong correlation between endocytosed PrP^C (small gold) and the immunolabeling with anti-PrP^C (large gold) on sections. Similar results were seen with the cells that were incubated for 10 min followed by the 50-min chase with protein A–gold (unpublished data), although more anti-PrP^C–gold was seen in late endocytic structures than in control cells (compare Fig. 1 F with Fig. S2 C). Quantitative analysis revealed that ~90% of the caveolae at the plasma membrane that were present after the 10-min incubation with protein A–gold at 37°C were still present after the 50-min chase.

To evaluate the rate of proteolysis of PrP^C after the 50-min chase, we performed Western blot analysis to measure the relative degradation of PrP^C before and after 1 h of protein A–gold uptake. Remarkably, no degradation was detected (Fig. S2 D). These data clearly show that PrP^C is internalized into nonclassical endosomes via caveolae and that this internalization is triggered by surrogate ligand protein A–gold. The rate of internalization is slow (<10% of all caveolae), and the triggered degradation of PrP^C is undetectable after 1 h "induced" internalization. Whether the triggered internalization is "cluster induced" could not be determined. A one-to-one relationship between a protein A molecule and a 5-nm gold particle is estimated, which argues for unclustered triggering. We observed that under steady state, PrP^C is also present in late endocytic multivesicular bodies (Fig. S1 F).

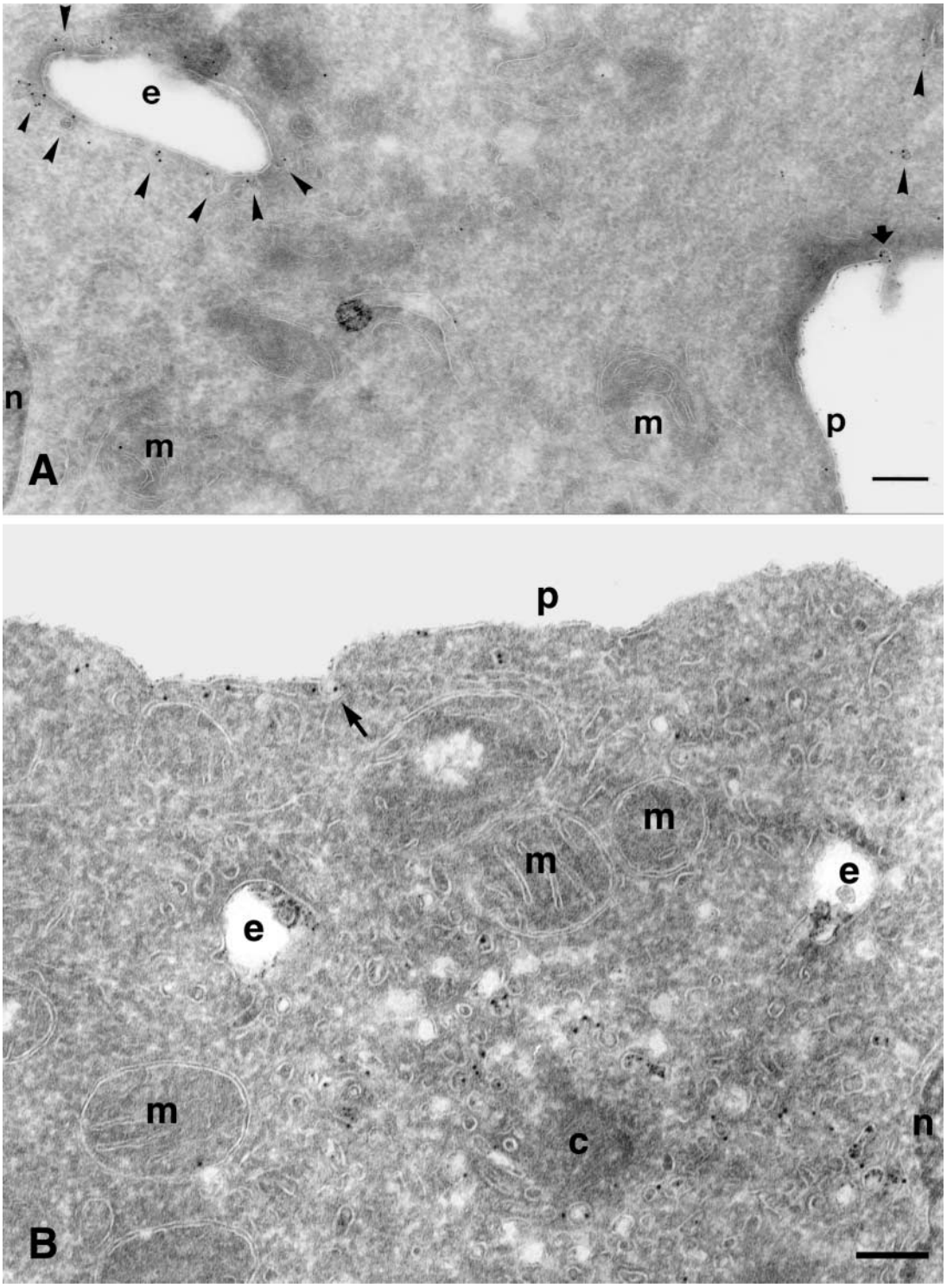

Figure 4. **Caveolae-mediated uptake of PrP^C is cholesterol dependent.** (A) PrP^C-dependent protein A–gold internalization in $SHaPrP^C$-expressing CHO/30C3 cells was temperature sensitive. Cells were preincubated with protein A–gold (5 nm) at 4°C before fixation. Ultrathin cryosections were labeled with an antibody against caveolin-1 (10-nm gold). Abundant protein A–gold was only seen on the plasma membrane and on plasma membrane–associated caveolae (thick arrow). Caveolin-1–positive endocytic structures (arrowheads) and caveolae-1 intracellular caveolae (arrowheads) did not exhibit any protein A–gold labeling (compare with Fig. 5). (B) Effect of filipin treatment on protein A–gold uptake and the fate of caveolae. Cells were treated for 24 h with filipin followed by a 10-min incubation in media that also contained protein A–gold (5 nm) and a 50-min chase at 37°C. Sections were labeled with anti–caveolin-1 (15 nm). A significant number of protein A–gold (small size) binding on the membrane was seen but no enrichment in caveolae (arrow). The uptake of protein A–gold is sharply reduced; endocytic structures contain protein A–gold (small size) at relatively low levels. No evidence of caveolae and no label for caveolin-1 (large gold) can be seen on these endocytic structures. Many caveolin-1–positive (large gold) vesicles/tubules are present in the pericentriolar region devoid of small protein A–gold. c, centriole; e, endocytic structure; m, mitochondria; n, nucleus; p, plasma membrane. Bars, 200 nm.

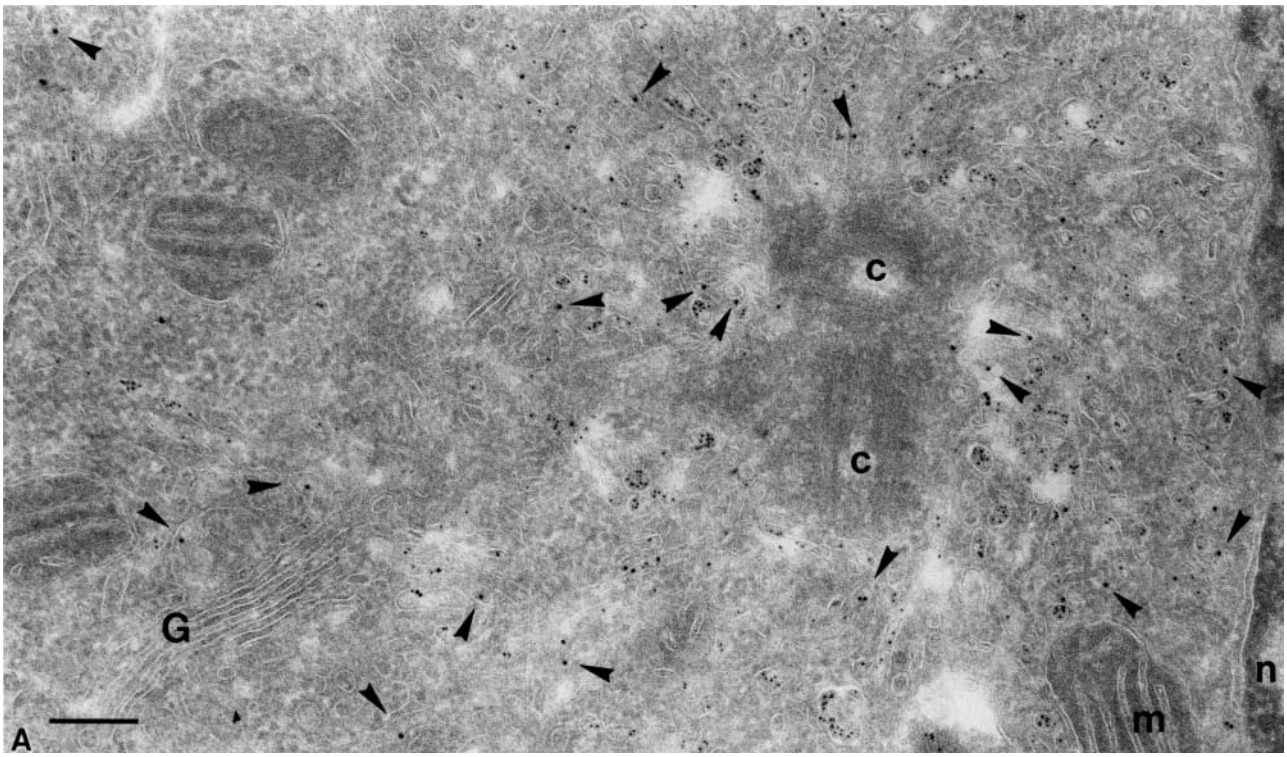

Figure 5. **Endocytosed protein A–gold was found in intracellular caveolae of SHaPrP^C-expressing CHO/30C3 cells that did not contain the transferrin receptor.** Cells were (A) incubated at 37°C for 10 min with 5-nm protein A–gold or (B) incubated at 37°C for 10 min with 5-nm protein A–gold and chased for 50 min before fixation. Ultrathin cryosections were labeled with antitransferrin antibodies (10-nm gold). (A) Protein A–gold (5 nm) detecting PrP^C labeling enriched in pericentriolar caveolae that did not colocalize with transferrin receptor–positive structures (10-nm gold, arrowheads). Panel B shows an identical result after a 50-min chase but with an accumulation of endocytosed protein A–gold in late endocytic multivesicular bodies. Transferrin receptor–positive labeling (10-nm gold) is found in endocytic structures that show an identical morphological appearance to PrP^C-containing structures. c, centriole; e, endocytic structure; G, Golgi complex; l, lysosomes; m, mitrochondria; n, nucleus; p, plasma membrane. Bars, 200 nm (also apply to Fig. 6).

Protein A–gold uptake is PrP^C dependent and sensitive to filipin

To determine whether protein A–gold uptake is dependent on PrP^C expression at the plasma membrane, CHO/30C3 and CHO/MH2M cells were treated with phosphatidylinositol-specific phospholipase C (PIPLC) at 37°C before incubation with protein A–gold to cleave GPI-linked PrP^C on the plasma membrane and endocytic compartments. Cryosections of these cells immunogold labeled with an α-PrP^C antibody showed no immunoreactivity for PrP^C on the plasma membrane or endosomal/lysosomal structures (Fig. 3). PrP^C labeling in ER and the Golgi complex (Fig. 3) remained unperturbed, confirming that PrP^C had been removed specifically from the plasma membrane, endosomes, and lysosomes by PIPLC. Furthermore, binding and uptake of protein A–gold on living cells was reduced to $<$0.1% (20 cells counted in treated and untreated cells; total $>$1,000 gold particles counted) after PIPLC treatment (Fig. 3), demonstrating that binding and uptake were dependent on the presence of PrP^C on the cell surface. PrP-deficient CHO/K1 and CHO/EV cells did not bind or endocytose protein A–gold (unpublished data), further emphasizing the specificity of binding by PrP^C to protein A–gold.

Several studies have indicated that raft-mediated uptake is sensitive to drugs that interfere in the homeostasis of cholesterol in the membrane lipid bilayer. We next analyzed whether treatment with filipin, a cholesterol-lowering agent, affects protein A–gold uptake and the fate of caveolae. When cells were treated for 24 h with filipin, followed by a 10-min incubation in media that also contained protein A–gold and a 50-min chase at 37°C, we found no significant reduction of protein A–gold binding on the plasma membrane. However, the presence of caveolae at the plasma membrane and the uptake of protein A–gold were sharply reduced (Fig. 4 B). Quantitative analysis of 20 random cross sections of cells revealed a 70% decrease in caveolae. In addition, endocytosed protein A–gold was only sparsely observed in endocytic structures. No evidence of caveolae and no label for caveolin were seen on these endocytic structures (Fig. 4 B). Caveolin-1 (large gold)–containing vesicles and tubules around the pericentriolar region did not contain endocytosed protein A–gold (small gold). See Fig. 2 D and Fig. 5 A for comparison in control cells. However, many caveolin-1–positive vesicles/tubules were identified in the pericentriolar region as in control cells (Fig. 2 D and Fig. 5 A). These data show that caveolae-mediated uptake of PrP^C is cholesterol dependent.

Caveolae on endocytic structures

To demonstrate unambiguously the association of endocytosed caveolae with endocytic structures, we compared uptake of protein A–gold binding to PrP^C at 4°C and at 37°C. If these caveolae-type "endocytic" structures label with pro-

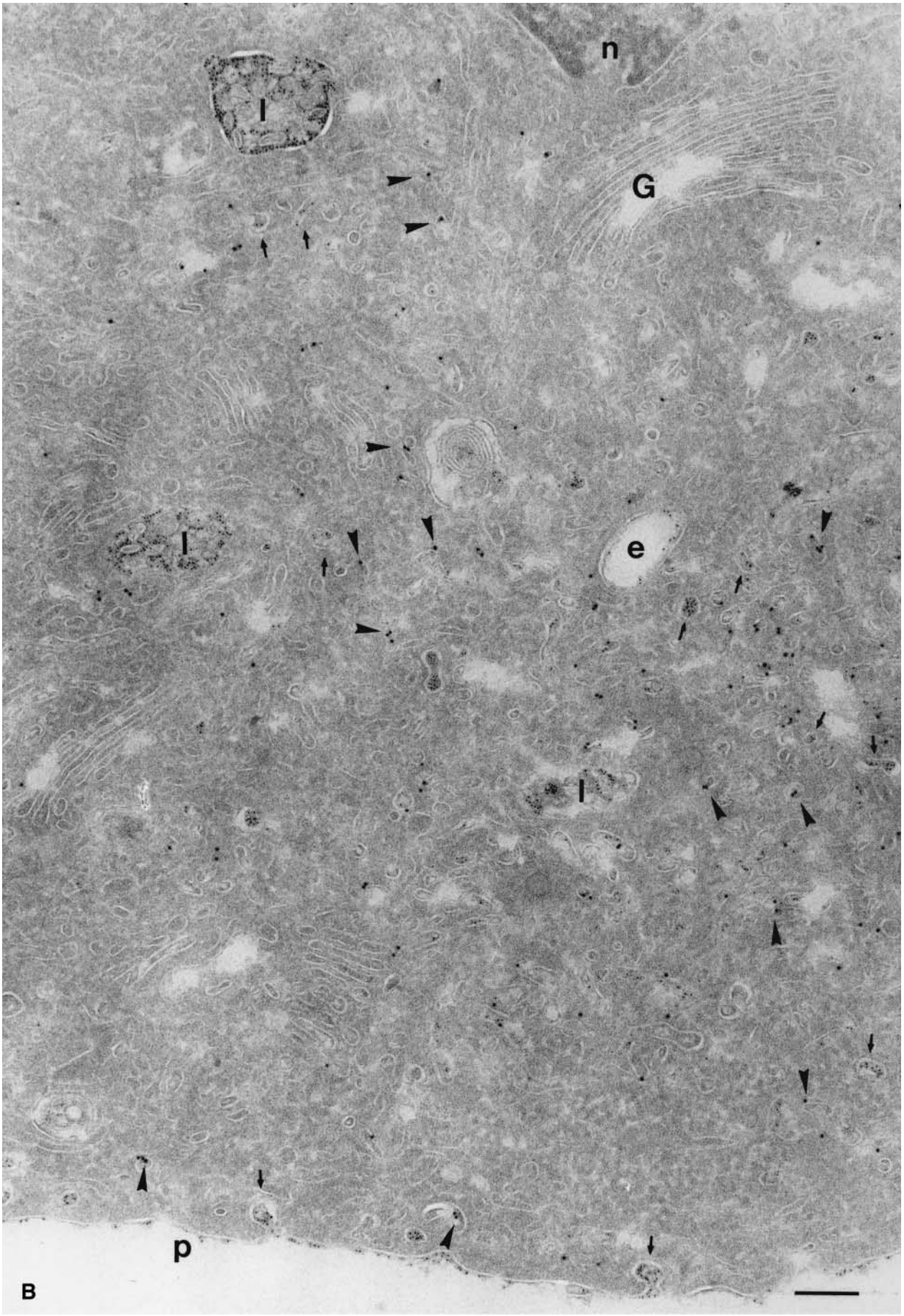

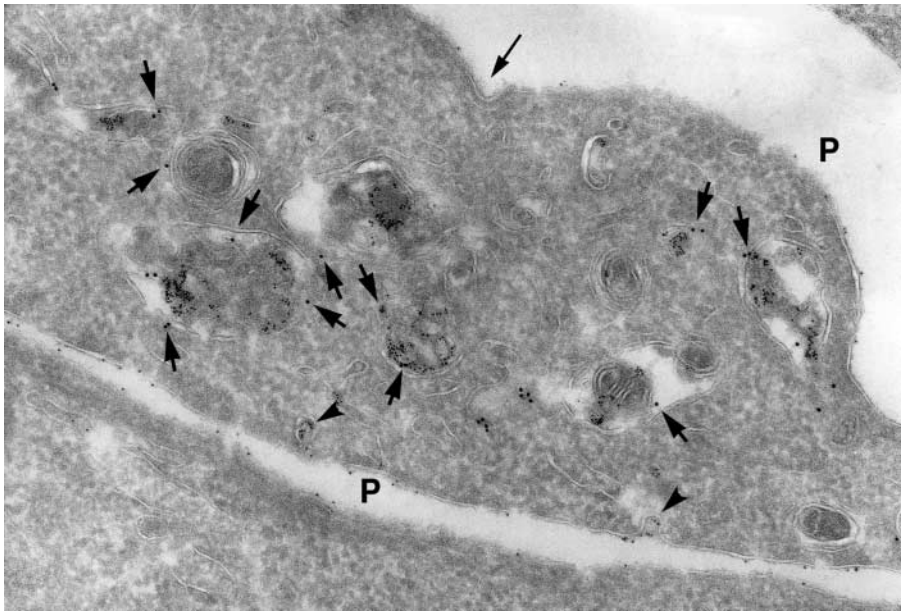

Figure 6. **Endocytosed protein A–gold accumulated in lysosomes of SHaPrP^C-expressing CHO/30C3 cells that contained the classical marker for late endocytic structures.** Cells were incubated at 37°C for 10 min with 5-nm protein A–gold and chased for 50 min before fixation. Ultrathin cryosections were labeled with anti–LGP-120 antibodies (15-nm gold). PrP^C labeling (protein A–gold, 5 nm) accumulated in LGP-120–positive structures. P, plasma membrane.

tein A–gold at 4°C, it would indicate that the structures were not endocytic but invaginations from the plasma membrane that are accessible to protein A–gold at 4°C. Cells were incubated for 10 min at either 4°C or 37°C with protein A–gold (5 nm), and the subcellular distribution of the gold was analyzed on cryosections. To analyze the distribution of caveolae, the sections were immunogold labeled with antibodies against caveolin-1 (10-nm gold).

We observed that at 4°C, protein A–gold bound to PrP^C in caveolae on the cell surface (Fig. 4 A, arrow). However, after analyzing >100 cells, no protein A–gold label was found in caveolae-associated endosomes that labeled for caveolin-1 (10-nm gold) (Fig. 4 A). In contrast, at 37°C, many caveolae-associated endocytic structures were loaded with protein A–gold bound to PrP^C (Fig. 2, C and D). Thus, structures labeled with protein A–gold, as described above (Fig. 1 F; Fig. 2, C–E; Fig. 6; and Fig. S2 C), were endocytic compartments containing internalized PrP^C. These experiments indicate that caveolae-associated endocytic structures exist and that efficient uptake of PrP^C into the caveolar endocytic pathway occurs only at physiological temperature.

Caveolae containing endocytosed PrP^C do not intersect with compartments containing the transferrin receptor and are delivered to late endosomal/lysosomal compartments via nonclassical endosomes

Previous studies have shown that the transferrin receptor is subject to endocytosis and recycling via clathrin-coated pits, early-sorting endosomes, and recycling endosomes. This early endocytic compartment has been well characterized in CHO cells (D'Souza-Schorey et al., 1998; Ghosh et al., 1998).

To investigate whether PrP^C endocytosed via caveolae intersects with the classical early endocytic recycling pathway, cells were subject to chase for 10 min or chase and pulse for 10 and 50 min, respectively, at 37°C with protein A–gold, and ultrathin cryosections were labeled using an antibody (H68-4) directed against the transferrin receptor. In sections of the 50-min pulse–treated cells, many tubulo-vesicular structures labeled with the transferrin receptor and were found next to the Golgi complex around the pericentriolar region (Fig. 5 A). Small protein A–gold particles were indicative of PrP^C molecules taken up via caveolae. Remarkably, in samples that had a high degree of ultrastructural preservation (Fig. 5 A), <2% of the small and large gold particles were present within the same vesicular structure. As soon as the ultrastructural preservation of cryosections was compromised, structures collapsed and could not be evaluated accurately. These results indicate that typical early endosomes do not intersect significantly with the endocytic pathway of PrP^C-containing caveolae.

To determine whether endocytosed PrP^C intersects with the transferrin receptor compartment on its way to late endosomes/lysosomes, we also evaluated the 50-min pulse period. In addition to the typical small tubulo-vesicular structures (Fig. 5 A) and swollen caveolae-type early endosomes, many larger multivesicular bodies ("late" endosomal/lysosomal profiles) were loaded with small gold particles representing endocytosed PrP^C, whereas the transferrin receptor (large gold) localized in nearby and distinct structures (Fig. 5 B). As expected, ER, Golgi complex, mitochondria, and nucleus were not labeled, indicating highly specific labeling in these experiments. To demonstrate that these findings were not induced by the protein A–gold uptake, we double labeled control cells with anti-PrP^C and transferrin receptor; no colocalization was seen for PrP^C and transferrin receptor (see Fig. S3, available at http://www.jcb.org/cgi/content/full/jcb.200304140/DC1). Based on these data, we conclude that PrP^C molecules endocytose via caveolae to larger endocytic structures and that this pathway does not intersect appreciably with the well-characterized, clathrin-mediated early endocytic recycling pathway of the transferrin receptor.

However, later during endocytosis, downstream of the early endocytic sorting/recycling pathway where transferrin resides, these PrP^C-loaded endocytic structures mix with typical late endocytic multivesicular bodies on their way to

lysosomes. To confirm the identity of these late endocytic structures, cells were labeled using an antibody against the lysosomal glycoprotein (LGP-120), a specific marker for these structures. Large gold (15 nm) anti–LGP-120 colocalized with the endocytosed (5 nm) protein A–gold, demonstrating the late endosomal/lysosomal distribution of endocytosed PrP^C (Fig. 6).

PrP^C follows a different route than other GPI-anchored proteins

Our data raise the question of whether other GPI-anchored proteins follow the same route as PrP^C in CHO cells. To address this question, we localized other GPI-anchored proteins in CHO cells. First, we used a CHO cell line stably expressing human GPI-anchored CD59 (Wheeler et al., 2002). The conditions of cell culture, fixation, and immunolabeling were identical to those described above for PrP^C. We found a uniform distribution of anti-CD59 on ER, Golgi complex, TGN (see Fig. S4 A, available at http://www.jcb.org/cgi/content/full/jcb.200304140/DC1), and the plasma membrane (Fig. S4, B and C), with a higher labeling density on the lamellae of the leading edge (not depicted) but without any enrichment in caveolae (Fig. S4 C). Furthermore, clathrin-coated pits at the plasma membrane (Fig. S4 B) were occasionally (~5% of 200 coated structures) labeled, and enrichment was seen at steady state in late endocytic multivesicular bodies (Fig. S4 B).

Next, we used the bacterial toxin aerolysin, which is a monovalent probe for the glycan core of several GPI-anchored proteins, to track the fate of a collection of GPI-anchored proteins (Fivaz et al., 2002). Remarkably, this probe does not bind GPI-anchored PrP^C (van der Goot, G., personal communication). Ultrathin cryosections of PrP^C-expressing CHO cells, as described above (Fig. 1, A–D), were incubated with biotinylated aerolysin followed by anti-biotin–gold. Moderate, but specific, labeling was seen on the plasma membrane, Golgi complex, and late endocytic multivesicular bodies (see Fig. S5 A, available at http://www.jcb.org/cgi/content/full/jcb.200304140/DC1), as described previously (Fivaz et al., 2002). We found a distinct, higher labeling intensity on plasma membrane lamellae (Fig. S5 B) and no detectable label in caveolae. A clathrin- and caveolin-independent pathway for internalization of CD59 or aerolysin probe could not be determined morphologically. These data confirm the differential sorting and fate of endocytosed GPI-anchored proteins described previously (Fivaz et al. 2002), including a different port of entry of PrP^C relative to other GPI-anchored proteins of the same cell type (this study).

Discussion

Caveolae in neurodegenerative disease

The localization of PrP^C in caveolae generates important questions about the physiological function of PrP^C and raises the possibility that caveolae are the site of pathological events that ultimately lead to prion disease. Caveolin-1 has been found in both serotonergic and noradrenergic neurons in culture as well as in cultured astrocytes, glial cells (Silva et al., 1999), and Schwann cells (Mikol et al., 1999). Caveolae have also been identified in astrocytes and endothelial cells in the brain and other tissues, such as intestine and muscle implicated in prion propagation and transmission (unpublished data). Significantly, interest in caveolae localization also has arisen from studies on trafficking and processing of amyloid precursor protein in Alzheimer's disease (Bouillot et al., 1996) and the colocalization of huntingtin with caveolin in caveolae in Huntington's disease (Peters et al., 2002). Thus, caveolae-type structures and rafts might be important subcellular structures for the manifestation of several neurodegenerative diseases.

PrP^C is internalized via the caveolar endosomal pathway

The ability of caveolae to internalize GPI-anchored proteins has been questioned because the GPI-anchored folate receptor and caveolin were not observed within endocytic structures under native conditions (Rothberg et al., 1990, 1992; van Deurs et al., 1993; Mayor et al., 1994). However, regulated internalization of caveolae has been demonstrated by morphological (Parton, 1994) and in vitro budding experiments (Schnitzer et al., 1996), by the presence of the motor protein dynamin on caveolae that mediates budding (Oh et al., 1998), and by activation of serum albumin receptor gp60, which triggers caveolae-uptake through Gi-dependent activation of the Src tyrosine kinase (Minshall et al., 2002). Important in this regard, the GPI anchor of PrP^C is modified with sialic acid, allowing PrP^C to reside in a different domain of the bilayer than either the folate receptor or Thy-1 (Rudd et al., 2001). This modification may account for the distinct endocytic properties attributed to PrP^C, although the exact mechanism of internalization remains to be determined. Our data concur with recently reported (Thomsen et al., 2002) findings that demonstrated using GFP-tagged caveolin-1 that caveolae are highly immobile plasma membrane microdomains. These authors concluded that caveolae are not involved in constitutive endocytosis but represent a highly stable plasma membrane compartment anchored by the actin cytoskeleton. However, our results show a low, but specific, level of dynamics and a clear presence of endocytic caveolae around the pericentriolar region and in nonclassical endocytic structures. The anchoring of cytoskeleton on caveolae was addressed using our EM analysis; bundles of actin (as close as 20 nm from caveolae) that are located parallel to the plasma membrane could be seen below some, but not all (<5%, 20 cells counted), caveolae. Specific distribution of actin was found around a minority of protein A–gold-containing caveolae (see Fig. S6, available at http://www.jcb.org/cgi/content/full/jcb.200304140/DC1). Antitubulin never showed any close association with caveolae at the plasma membrane (unpublished data).

Our findings explain earlier reports on the redistribution and clustering of GPI-anchored proteins in caveolae and lead us to suggest that caveolae are specific organelles for endocytosis (Ying et al., 1992; Sargiacomo et al., 1993; Smart et al., 1995). This hypothesis is supported by several studies. First, Pelkmans et al. (2001) described the caveolar endocytosis of SV40 into unique, large peripheral organelles,

termed caveosomes, containing neither the classical endosomal markers nor ligands of clathrin-coated vesicles. If caveosomes, as described by Pelkmans et al. (2001), are defined as endocytic compartments that receive caveolin-decorated vesicles from the plasma membrane irrespective of SV40 virus, then these nonclassical endosomes can be considered caveosomes. Further investigation will clarify whether these virus-induced caveosomes are similar to the caveolar endocytosis into nonclassic endocytic structures that we observed for endocytosed PrP^C. Second, Nichols et al. (2001) described a similar pathway taken by a GPI-tagged GFP and also reported the continuous microtubule- and temperature-dependent cycling of GPI-linked GFP and GPI-linked CD59 between the cell surface and trans-Golgi that was independent of clathrin endocytic machinery. Lamaze et al. (2001) described the internalization of the lipid raft–associated interleukin 2 receptor in T cells lacking caveolin-1 via a novel mechanism independent of clathrin and dependent upon dynamin. We never found PrP^C to be enriched in clathrin-coated pits in brain (Mironov et al., 2003). Together, these observations support the hypothesis that two distinct nonclathrin uptake mechanisms exist that are both detergent resistant and dynamin dependent. One mechanism is clearly caveolar and the other is of noncoated origin. Each pathway is associated with unique G proteins (Oh and Schnitzer, 2001).

The active internalization of PrP^C via caveolae raises new questions in the study of prion biology. For example, does the reported signaling activity of PrP^C occur at the plasma membrane or after caveolae-mediated endocytosis (Mouillet-Richard et al., 2000)? Similarly, is endocytosis via caveolae a necessary step in the conversion of PrP^C into PrP^{Sc}, perhaps because of a change in milieu or in the relative concentration of PrP conformers or other auxiliary molecules involved in prion propagation (Telling et al., 1995)? Is the role of PrP^{Sc} in promoting neuronal cell dysfunction performed during or after endocytosis? Is the caveolin-knockout mouse resistant to oral prion infection? Future studies of this internalization pathway may lead to the identification of inhibitors of the caveolae-mediated endocytosis of PrP^C, and such molecules may be useful as reagents for the treatment of prion diseases and other neurodegenerative disorders.

Materials and methods

Chemicals and reagents

Protein A–gold, 5-nm gold particles coupled to protein A molecules in a 1:1 anticipated ratio, was produced by J. Griffiths from the Utrecht University Medical School Department of Cell Biology.

Cultured cells

Production of CHO cells expressing $SHaPrP^C$ (CHO/30C3) was reported previously (Blochberger et al., 1997).

Antibodies and purified PrP^C

For all studies described here, data using Fab R1 are shown. Identical results were obtained with R2, D13, and Fab D18, which recognizes residues 133–157 (Peretz et al., 1997; Williamson et al., 1998). The mAb against caveolin-1 was a gift from M. Lisanti (Albert Einstein College, New York, NY). See supplemental Materials and methods (available at http://www.jcb.org/cgi/content/full/jcb.200304140/DC1) for more details of other antibodies and purified PrP^C.

Binding studies

Binding of labeled conjugates was performed on the different cells in culture and on purified proteins immobilized on nitrocellulose. Confluent cells were washed with media twice before incubation for 1 h with media containing protein A–gold (OD 0.3). See supplemental Materials and methods for more details.

Immunogold labeling of living cells

To study uptake of protein A–gold, the different cell lines were incubated for 10 min with media containing protein A–gold and then fixed or chased for an additional 50 min at 37°C before fixation. See supplemental Materials and methods for more details.

Cryoimmunogold electron microscopy

Subcellular localization of antigens using high-resolution cryoimmunogold electron microscopy was performed as previously described (Peters and Hunziker, 2001). See supplemental Materials and methods for more details.

Online supplemental material

The supplemental material (Figs. S1–S6 and supplemental Materials and methods) is available at http://www.jcb.org/cgi/content/full/jcb.200304140/DC1. A concise description of the data presented in each supplemental figure is introduced upon citation in the text. Further comments on the data reported can be found in the online legends. Methodological details (including the Western blotting procedure) that are not necessary for understanding the logic and structure of the experiments have been relegated to the supplemental Materials and methods.

We thank Drs. Crislyn D'Souza Schorey, Hans Geuze, Jan Slot, Sjaak Neefjes, Ton Berns, and Holger Wille for critical suggestions during the course of the study. We also acknowledge the photography departments of the Cell Biology Department in Utrecht and Amsterdam for their darkroom work. Hang Nguyen and Reilly O'Neal were very valuable with editing this manuscript.

This work was supported by grants from the National Institutes of Health (AG02132 and AG010770) to Dr. Stanley Prusniner and the European Union, Framework Program 5, grant QLRT 2001-01628.

Submitted: 25 April 2003
Accepted: 30 June 2003

References

Anderson, R.G. 1998. The caveolae membrane system. *Annu. Rev. Biochem.* 67: 199–225.

Arnold, J.E., C. Tipler, L. Laszlo, J. Hope, M. Landon, and R.J. Mayer. 1995. The abnormal isoform of the prion protein accumulates in late-endosome-like organelles in scrapie-infected mouse brain. *J. Pathol.* 176:403–411.

Blochberger, T.C., C. Cooper, D. Peretz, J. Tatzelt, O.H. Griffith, M.A. Baldwin, and S.B. Prusiner. 1997. Prion protein expression in Chinese hamster ovary cells using a glutamine synthetase selection and amplification system. *Protein Eng.* 10:1465–1473.

Borchelt, D.R., M. Scott, A. Taraboulos, N. Stahl, and S.B. Prusiner. 1990. Scrapie and cellular prion proteins differ in their kinetics of synthesis and topology in cultured cells. *J. Cell Biol.* 110:743–752.

Bouillot, C., A. Prochiantz, G. Rougon, and B. Allinquant. 1996. Axonal amyloid precursor protein expressed by neurons in vitro is present in a membrane fraction with caveolae-like properties. *J. Biol. Chem.* 271:7640–7644.

Brown, D.A., and K. Jacobson. 2001. Microdomains, Lipid Rafts and Caveolae (San Feliu de Guixols, Spain, 19-24 May 2001). *Traffic.* 2:668–672.

Caughey, B., and G.J. Raymond. 1991. The scrapie-associated form of PrP is made from a cell surface precursor that is both protease- and phospholipase-sensitive. *J. Biol. Chem.* 266:18217–18223.

Conner, S.D., and S.L. Schmid. 2003. Regulated portals of entry into the cell. *Nature.* 422:37–46.

D'Souza-Schorey, C., E. van Donselaar, V.W. Hsu, C. Yang, P.D. Stahl, and P.J. Peters. 1998. ARF6 targets recycling vesicles to the plasma membrane: insights from an ultrastructural investigation. *J. Cell Biol.* 140:603–616.

Fivaz, M., F. Vilbois, S. Thurnheer, C. Pasquali, L. Abrami, P.E. Bickel, R.G. Parton, and F.G. van der Goot. 2002. Differential sorting and fate of endocytosed GPI-anchored proteins. *EMBO J.* 21:3989–4000.

Ghosh, R.N., W.G. Mallet, T.T. Soe, T.E. McGraw, and F.R. Maxfield. 1998. An endocytosed TGN38 chimeric protein is delivered to the TGN after traffick-

ing through the endocytic recycling compartment in CHO cells. *J. Cell Biol.* 142:923–936.

Gorodinsky, A., and D.A. Harris. 1995. Glycolipid-anchored proteins in neuroblastoma cells form detergent-resistant complexes without caveolin. *J. Cell Biol.* 129:619–627.

Harmey, J.H., D. Doyle, V. Brown, and M.S. Rogers. 1995. The cellular isoform of the prion protein, PrP^{C}, is associated with caveolae in mouse neuroblastoma (N2a) cells. *Biochem. Biophys. Res. Commun.* 210:753–759.

Kaneko, K., M. Vey, M. Scott, S. Pilkuhn, F.E. Cohen, and S.B. Prusiner. 1997. COOH-terminal sequence of the cellular prion protein directs subcellular trafficking and controls conversion into the scrapie isoform. *Proc. Natl. Acad. Sci. USA.* 94:2333–2338.

Kurzchalia, T.V., and R.G. Parton. 1999. Membrane microdomains and caveolae. *Curr. Opin. Cell Biol.* 11:424–431.

Lamaze, C., A. Dujeancourt, T. Baba, C.G. Lo, A. Benmerah, and A. Dautry-Varsat. 2001. Interleukin 2 receptors and detergent-resistant membrane domains define a clathrin-independent endocytic pathway. *Mol. Cell.* 7:661–671.

Madore, N., K.L. Smith, C.H. Graham, A. Jen, K. Brady, S. Hall, and R. Morris. 1999. Functionally different GPI proteins are organized in different domains on the neuronal surface. *EMBO J.* 18:6917–6926.

Mayor, S., K.G. Rothberg, and F.R. Maxfield. 1994. Sequestration of GPI-anchored proteins in caveolae triggered by cross-linking. *Science.* 264:1948–1951.

McKinley, M.P., A. Taraboulos, L. Kenaga, D. Serban, A. Stieber, S.J. DeArmond, S.B. Prusiner, and N. Gonatas. 1991. Ultrastructural localization of scrapie prion proteins in cytoplasmic vesicles of infected cultured cells. *Lab. Invest.* 65:622–630.

Mikol, D.D., H.L. Hong, H.L. Cheng, and E.L. Feldman. 1999. Caveolin-1 expression in Schwann cells. *Glia.* 27:39–52.

Minshall, R.D., C. Tiruppathi, S.M. Vogel, and A.B. Malik. 2002. Vesicle formation and trafficking in endothelial cells and regulation of endothelial barrier function. *Histochem. Cell Biol.* 117:105–112.

Mironov, A., Jr., D. Latawiec, H. Wille, E. Bouzamondo, G. Legname, R.A. Williamson, S.J. DeArmond, S.B. Prusiner, and P.J. Peters. 2003. Cytosolic prion protein in neurons. *J. Neurosci.* In press.

Mouillet-Richard, S., M. Ermonval, C. Chebassier, J.L. Laplanche, S. Lehmann, J.M. Launay, and O. Kellermann. 2000. Signal transduction through prion protein. *Science.* 289:1925–1928.

Naslavsky, N., R. Stein, A. Yanai, G. Friedlander, and A. Taraboulos. 1997. Characterization of detergent-insoluble complexes containing the cellular prion protein and its scrapie isoform. *J. Biol. Chem.* 272:6324–6331.

Nichols, B.J., A.K. Kenworthy, R.S. Polishchuk, R. Lodge, T.H. Roberts, K. Hirschberg, R.D. Phair, and J. Lippincott-Schwartz. 2001. Rapid cycling of lipid raft markers between the cell surface and Golgi complex. *J. Cell Biol.* 153:529–541.

Oesch, B., D. Westaway, M. Wälchli, M.P. McKinley, S.B.H. Kent, R. Aebersold, R.A. Barry, P. Tempst, D.B. Teplow, L.E. Hood, et al. 1985. A cellular gene encodes scrapie PrP 27-30 protein. *Cell.* 40:735–746.

Oh, P., and J.E. Schnitzer. 2001. Segregation of heterotrimeric G proteins in cell surface microdomains. G(q) binds caveolin to concentrate in caveolae, whereas G(i) and G(s) target lipid rafts by default. *Mol. Biol. Cell.* 12:685–698.

Oh, P., D.P. McIntosh, and J.E. Schnitzer. 1998. Dynamin at the neck of caveolae mediates their budding to form transport vesicles by GTP-driven fission from the plasma membrane of endothelium. *J. Cell Biol.* 141:101–114.

Pan, K.-M., M. Baldwin, J. Nguyen, M. Gasset, A. Serban, D. Groth, I. Mehlhorn, Z. Huang, R.J. Fletterick, F.E. Cohen, and S.B. Prusiner. 1993. Conversion of α-helices into β-sheets features in the formation of the scrapie prion proteins. *Proc. Natl. Acad. Sci. USA.* 90:10962–10966.

Parton, R.G. 1994. Ultrastructural localization of gangliosides; GM_1 is concentrated in caveolae. *J. Histochem. Cytochem.* 42:155–166.

Parton, R.G. 2003. Caveolae - from ultrastructure to molecular mechanisms. *Nat. Rev. Mol Cell Biol.* 4:162–167.

Pelkmans, L., J. Kartenbeck, and A. Helenius. 2001. Caveolar endocytosis of simian virus 40 reveals a new two-step vesicular-transport pathway to the ER. *Nat. Cell Biol.* 3:473–483.

Peretz, D., R.A. Williamson, Y. Matsunaga, H. Serban, C. Pinilla, R.B. Bastidas, R. Rozenshteyn, T.L. James, R.A. Houghten, F.E. Cohen, et al. 1997. A conformational transition at the N terminus of the prion protein features in formation of the scrapie isoform. *J. Mol. Biol.* 273:614–622.

Peters, P.J., and W. Hunziker. 2001. Subcellular localization of Rab17 by cryo-immunogold electron microscopy in epithelial cells grown on polycarbonate filters. *Methods Enzymol.* 329:210–225.

Peters, P.J., K. Ning, F. Palacios, R.L. Boshans, A. Kazantsev, L.M. Thompson, B. Woodman, G.P. Bates, and C. D'Souza-Schorey. 2002. Arfaptin 2 regulates the aggregation of mutant huntingtin protein. *Nat. Cell Biol.* 4:240–245.

Prusiner, S.B. 1994. Biology and genetics of prion diseases. *Annu. Rev. Microbiol.* 48:655–686.

Rothberg, K.G., Y. Ying, J.F. Kolhouse, B.A. Kamen, and R.G.W. Anderson. 1990. The glycophospholipid-linked folate receptor internalizes folate without entering the clathrin-coated pit endocytic pathway. *J. Cell Biol.* 110: 637–649.

Rothberg, K.G., J.E. Heuser, W.C. Donzell, Y.S. Ying, J.R. Glenney, and R.G. Anderson. 1992. Caveolin, a protein component of caveolae membrane coats. *Cell.* 68:673–682.

Rudd, P.M., M.R. Wormald, D.R. Wing, S.B. Prusiner, and R.A. Dwek. 2001. Prion glycoprotein: structure, dynamics, and roles for the sugars. *Biochemistry.* 40:3759–3766.

Sargiacomo, M., M. Sudol, Z. Tang, and M.P. Lisanti. 1993. Signal transducing molecules and glycosyl-phosphatidylinositol–linked proteins from a caveolin-rich insoluble complex in MDCK cells. *J. Cell Biol.* 122:789–807.

Scherfeld, D., G. Schneider, P. Guttmann, and M. Osborn. 1998. Visualization of cytoskeletal elements in the transmission X-ray microscope. *J. Struct. Biol.* 123:72–82.

Schnitzer, J.E., P. Oh, and D.P. McIntosh. 1996. Role of GTP hydrolysis in fission of caveolae directly from plasma membranes. *Science.* 274:239–242.

Silva, W.I., H.M. Maldonado, M.P. Lisanti, J. Devellis, G. Chompre, N. Mayol, M. Ortiz, G. Velazquez, A. Maldonado, and J. Montalvo. 1999. Identification of caveolae and caveolin in C6 glioma cells. *Int. J. Dev. Neurosci.* 17:705–714.

Simons, K., and E. Ikonen. 1997. Functional rafts in cell membranes. *Nature.* 387: 569–572.

Smart, E.J., Y.-S. Ying, C. Mineo, and R.G.W. Anderson. 1995. A detergent-free method for purifying caveolae membrane from tissue culture cells. *Proc. Natl. Acad. Sci. USA.* 92:10104–10108.

Taraboulos, A., D. Serban, and S.B. Prusiner. 1990. Scrapie prion proteins accumulate in the cytoplasm of persistently infected cultured cells. *J. Cell Biol.* 110:2117–2132.

Taraboulos, A., M. Scott, A. Semenov, D. Avrahami, L. Laszlo, and S.B. Prusiner. 1995. Cholesterol depletion and modification of COOH-terminal targeting sequence of the prion protein inhibits formation of the scrapie isoform. *J. Cell Biol.* 129:121–132.

Telling, G.C., M. Scott, J. Mastrianni, R. Gabizon, M. Torchia, F.E. Cohen, S.J. DeArmond, and S.B. Prusiner. 1995. Prion propagation in mice expressing human and chimeric PrP transgenes implicates the interaction of cellular PrP with another protein. *Cell.* 83:79–90.

Thomsen, P., K. Roepstorff, M. Stahlhut, and B. van Deurs. 2002. Caveolae are highly immobile plasma membrane microdomains, which are not involved in constitutive endocytic trafficking. *Mol. Biol. Cell.* 13:238–250.

van Deurs, B., P.K. Holm, L. Kayser, K. Sandvig, and S.H. Hansen. 1993. Multivesicular bodies in HEp-2 cells are maturing endosomes. *Eur. J. Cell Biol.* 61:208–224.

Vey, M., S. Pilkuhn, H. Wille, R. Nixon, S.J. DeArmond, E.J. Smart, R.G. Anderson, A. Taraboulos, and S.B. Prusiner. 1996. Subcellular colocalization of the cellular and scrapie prion proteins in caveolae-like membranous domains. *Proc. Natl. Acad. Sci. USA.* 93:14945–14949.

Wheeler, S.F., P.M. Rudd, S.J. Davis, R.A. Dwek, and D.J. Harvey. 2002. Comparison of the N-linked glycans from soluble and GPI-anchored CD59 expressed CHO cells. *Glycobiology.* 12:261–271.

Wille, H., M.D. Michelitsch, V. Guenebaut, S. Supattapone, A. Serban, F.E. Cohen, D.A. Agard, and S.B. Prusiner. 2002. Structural studies of the scrapie prion protein by electron crystallography. *Proc. Natl. Acad. Sci. USA.* 99: 3563–3568.

Williamson, R.A., D. Peretz, C. Pinilla, H. Ball, R.B. Bastidas, R. Rozenshteyn, R.A. Houghten, S.B. Prusiner, and D.R. Burton. 1998. Mapping the prion protein using recombinant antibodies. *J. Virol.* 72:9413–9418.

Ying, Y.-S., R.G.W. Anderson, and K.G. Rothberg. 1992. Each caveola contains multiple glycosyl-phosphatidylinositol-anchored membrane proteins. *Cold Spring Harb. Symp. Quant. Biol.* 57:593–604.